Measurement of the acoustic properties of amorphous silica above 4.5 mK

E. Nazaretski,[1,2] R. D. Merithew,[1] R. O. Pohl,[1] and J. M. Parpia[1]
[1]*Laboratory of Atomic and Solid State Physics, Cornell University, Ithaca, New York 14853, USA*
[2]*Los Alamos National Laboratory, Los Alamos, New Mexico 87545, USA*
(Received 29 August 2004; published 1 April 2005)

Measurements of speed of sound and internal friction of a-SiO_2 were extended down to ≈4 mK (sample temperature) in a cryostat shielded with lead against γ radiation. We conclude that the sample starts to thermally decouple below 8 mK primarily due to internal heat release. Down to 10 mK, the speed of sound is shown to be compatible with the predictions of the tunneling model, with no evidence seen for a low energy cut-off of the tunnel splitting, contrary to our earlier claims.

DOI: 10.1103/PhysRevB.71.144201 PACS number(s): 61.43.Fs, 63.50.+x, 62.40.+i

I. INTRODUCTION

Since the work by Debye, Born, and von Karman, it has been known that the lattice vibrations of crystals are described by elastic waves. It is also known that lattice defects in crystals can lead to spatially localized impurity modes that depend critically on the type of disorder.[1] Defect modes have also been detected in amorphous solids. However, those are independent of the chemical composition and preparation of these solids, as evidenced by their thermal and elastic properties that are qualitatively indistinguishable and quantitatively identical to within an order of magnitude.[2] In the energy range of 10^{-3} eV and below, these modes have been successfully described by the tunneling model (TM),[3,4] reviewed in Ref. 5, which postulates the existence of atoms or groups of atoms that tunnel at low temperatures between nearly equivalent equilibrium positions. In the TM, the tunneling defects are assumed not to interact with each other. Evidence of deviations from the TM has been reported by Classen *et al.*[6] and has been interpreted in terms of tunneling defect interactions.[7]

In an investigation of the speed of sound of amorphous silica, a deviation from the behavior expected on the basis of the TM was reported by us below 25 mK which could be described phenomenologically by a low energy cutoff, $\Delta_{0,min}$ of the tunneling splitting.[8] Two other unexpected observations were reported in this paper. Discontinuous jumps in the frequency traces of the oscillator had been observed below 12 mK, along with evidence for nonlinear oscillations as the strain amplitude was increased. These two observations have since found simple explanations. Classen *et al.* observed that the nonlinear oscillations were the result of strain-induced heating,[9] while the noise in the frequency traces at the lowest temperatures has been understood as originating in an interaction between the two level systems and low level radioactivity as well as via bombardment by cosmic rays.[10,11] In the present publication it will be shown that the measurements provide no evidence for the existence of a low-energy cutoff of the tunneling splitting, contrary to our earlier conclusion.[8] By extending the earlier work to 4.5 mK, we have identified long term heat release and heating due to cosmic rays as two contributing sources of power that result in an elevation of the sample temperature above ambient, leading to a temperature dependence of the sound velocity similar to that expected for a finite $\Delta_{0,min}$.

II. EXPERIMENT

A. Cryostat and sample

The torsional oscillator was mounted on a dilution refrigerator equipped with a $PrNi_5$ nuclear stage. A ^{3}He melting curve thermometer calibrated to the ^{3}He solid transition that occurs at 0.9 mK was used to monitor the temperature of the experimental plate. To minimize the vibrations of the cryostat it was decoupled from the floor through air legs. Special care was taken when grounding electronic devices to minimize rf pickup to the experiment. A more detailed description of the cryostat can be found elsewhere.[12] Data were taken over the temperature range (registered on the melting curve thermometer) between 0.9 and 100 mK. A high precision power supply was used to vary the current in the demagnetization magnet. This allowed us to control the temperature of the experimental plate with an accuracy better than a fraction of a μK below 10 mK. We used 5 cm thick lead bricks to shield the cryostat against ambient radioactivity in the cryostat surroundings, as described elsewhere.[13]

The amorphous silica sample in the oscillator, Suprasil-W ($<$5 ppm OH^- impurities; see also Table 1, Ref. 2) was the same as the one studied previously,[8] 2.23 cm long, 0.40 cm diameter, with rough faces at both ends. Since it still carried the Dale thermometer with the leads glued to it, as used in the earlier work (see Fig. 1 of Ref. 8) the sample had to be removed from the base and cleaned. A visual inspection showed that its surface appeared rough. Thereafter, the sample was reattached to the quartz transducer (length: 2.2 cm) using Stycast 2850FT (for each joint, a ~0.5 mg drop was used).[14] This amount had previously been overestimated by a factor of 10.[15] As in the previous study, the oscillator was encased in a Nb tube (d=0.635 cm, 0.05 cm wall thickness, l=6.0 cm) to maintain the sample at approximately the Earth's magnetic field.

B. Torsional oscillator measurements

The response of the oscillator was acquired with a lock in amplifier and a frequency synthesizer whose frequency could be swept around the resonance (range ≈±0.5 Hz) at a constant temperature in 2000 seconds, sufficiently slow so as not to significantly skew the resonant frequency due to the oscil-

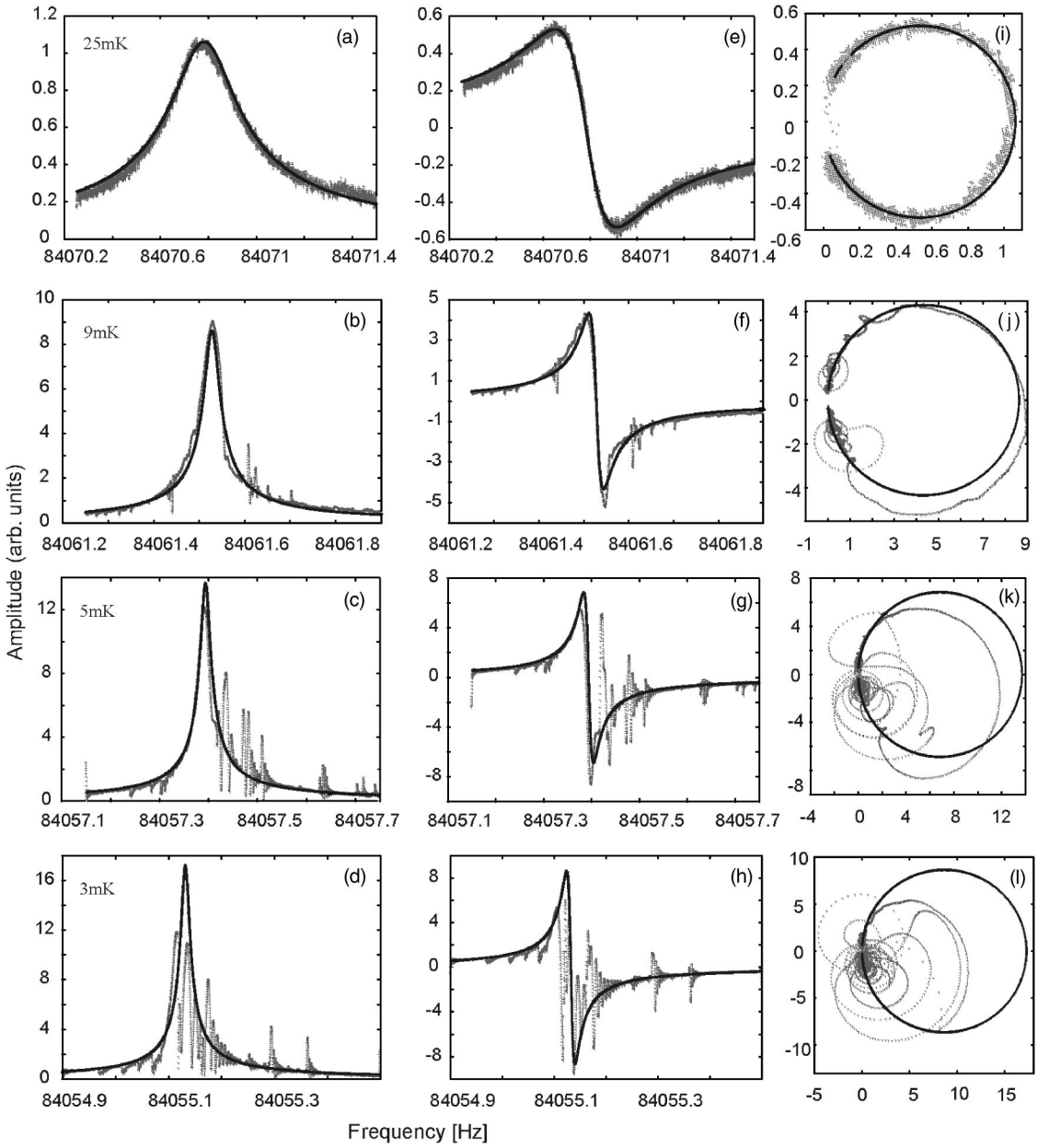

FIG. 1. Frequency traces. Left column (panels a–d): vector amplitude (voltage) registered by the lock-in amplifier. Middle column (panels e–h): The real part of the signal and right column (i–l) phase (Nyquist) plot. The spikes are caused by μ irradiation hitting the oscillator with a frequency of 0.025/s. Note that their effect is not symmetrical, in particular as shown in the vector signal (Ref. 10). The solid lines are fits as described in the text. 1 arb. unit corresponds to a strain, $\epsilon_a = 1.39 \times 10^{-10}$ (Ref. 16). Temperatures are those of the experimental plate.

lator time constant ($\sim$30 s at the lowest temperatures). The resonant frequency of the composite oscillator was then converted into the speed of sound of the a-SiO_2 sample by following the procedure described by Topp.[15] Note that in the experimental results shown in Fig. 1, we plot the frequency of the torsional oscillator, while the changes in the sound velocities $(\Delta V(T)/V_0)$ shown later are those of the amorphous sample. To convert the observed damping to an internal friction of the sample, we ascribed the entire damping to the a-SiO_2 sample, as explained by Topp.[15]

To allow a comparison with other experiments it was necessary to calibrate the amplitude of the oscillations so that the piezoelectric signal caused by the quartz transducer could be converted into the strain amplitude of the a-SiO_2. We reflected a laser beam off a mirror attached to the sample at room temperature and used a movable photodiode to measure the reflected beam profile. A measurement of the profile with the oscillator at rest, combined with a lock-in measurement of the ac component of the photodiode signal with the oscillator driven on resonance was used to determine the absolute angular displacement of the end of the composite oscillator.[16] The strain amplitude (ε_a) is defined as one half of the maximum angular displacement between the two ends of the a-SiO_2 cylinder. The resonances described here were

mapped with peak strain amplitudes as low as 10^{-9}, except for strain heating experiments where strains as high as 10^{-7} were used (see Fig. 5, later).

Typical frequency sweeps at four different temperatures are shown in Fig. 1. In the left column we show the amplitude versus the drive frequency, in the middle column we show the in-phase response, and on the right are plotted the in-phase component (on the abscissas) versus the out-of-phase component, generating a phase (Nyquist) plot. The solid lines are fits to the amplitude of oscillation using the so-called double Lorentzian form given in Eq. (1):

$$A(f_d) = (\tau/4\pi^2 I)/((f_0^2 - f_d^2)^2 + (f_0 f_d/Q)^2)^{1/2}. \quad (1)$$

Here τ is the drive torque, I the moment of inertia of the oscillator, f_0 the resonant frequency, f_d the drive frequency, and Q is the quality factor, defined as the full width at half-power [or the width at $A(f_0)/\sqrt{2}$]. Above 25 mK, these fits are seen to be nearly perfect. At 9 mK, we clearly see the onset of transients, evidence for the effect of cosmic ray muons (μ), as discussed in Ref. 10. In Ref. 11 we describe the effects of interactions with ambient γ irradiation. While γ quanta can be shielded out by a 5 cm thick lead wall around the cryostat, the "hard" component of the cosmic rays [consisting of high energy μ (Refs. 17 and 18)] cannot be shielded out by the lead. In fitting the data, we paid particular attention to frequencies away from resonance since the transients are not as pronounced there. The fits are still good even at an experimental plate temperature of 3 mK, although the transients close to f_0 tend to mask the Lorentzian shapes, and the Nyquist plots are greatly affected by them. f_0 together with the internal friction Q^{-1}, were determined from the Lorentzian fits to the amplitude traces and the real part (The middle column in Fig. 1).

III. EXPERIMENTAL RESULTS

A. Time dependence of the sound velocity

Once the cryostat was shielded by erecting the lead cave around it, we were able to map out the resonances as shown in Fig. 1. We carried out measurements of the sound velocity over experimental plate temperatures between 1 and 100 mK to reproduce and extend our earlier measurements.[8] Systematic measurements now revealed the unexpected result that at a stage temperature below $\approx$8 mK, the sound velocity $[\Delta V(T)/V_0]$ in the a-SiO_2 decreased with increasing time, as shown in Figs. 2 and 3. Evidently, the sample was not in thermal equilibrium with the stage, and continued to cool, even after several months. This can only be explained as slow thermal relaxation, a phenomenon well known in amorphous solids, previously measured only for times less than 200 h.[19–21]. The heat released in the amorphous sample causes thermal decoupling from the stage. Within the TM it can be explained through a slow thermalization of the tunneling defects. Figure 2 also shows how an increased heating of the sample (i.e., at earlier times) primarily affects the low temperature data without changing the higher temperature $\Delta V(T)/V_0$ dependence. This observation will be pursued further later (Fig. 7).

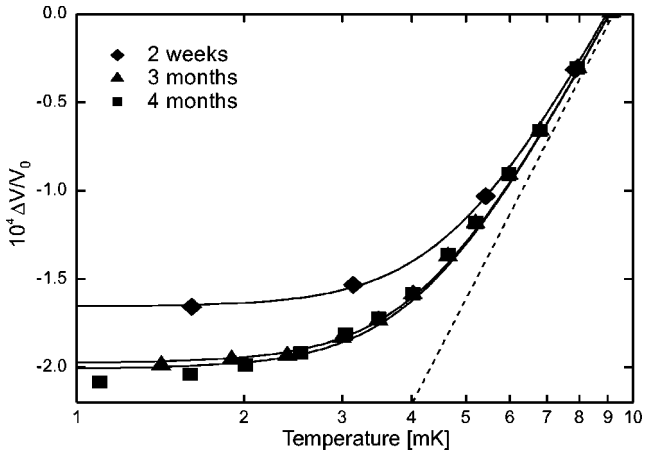

FIG. 2. Resonance frequency converted to changes in the sound velocity of the amorphous sample, against the temperature of the experimental plate. Below 10 mK the sound velocity exhibits a long-term time dependence, attributed to heat evolution from the relaxation of the tunneling states in the a-SiO_2. Data were acquired two weeks (diamonds), three months (triangles), and four months (squares) after the transfer of helium. The dashed line [Eq. (2)] is the same as that discussed in Fig. 4. The solid curves are discussed in Sec. III A.

Figure 4 shows that between 10 mK and 80 mK, the speed of sound varies logarithmically with temperature as predicted by the standard tunneling model. A fit to the data yields the change in the sound velocity, $\Delta V(T)/V_0$,

$$\Delta V(T)/V_0 = C_0 \ln(T/T_0) = 2.65 \times 10^{-4} \ln(T/T_0), \quad (2)$$

where V_0 is the sound velocity at some reference temperature (T_0=9.2 mK in Fig. 2), and C_0 is the so-called tunneling strength.

The previously published results (see Fig. 4) show a deviation from the $\ln T$ dependence (indicated as the dashed line) that commences at $\sim$25 mK rather than at $\sim$8 mK for the present data set, which we attribute to the temperature stabilization procedure used in the earlier experiment.[22] The deviation had been interpreted as evidence for a $\Delta_{0,min}$

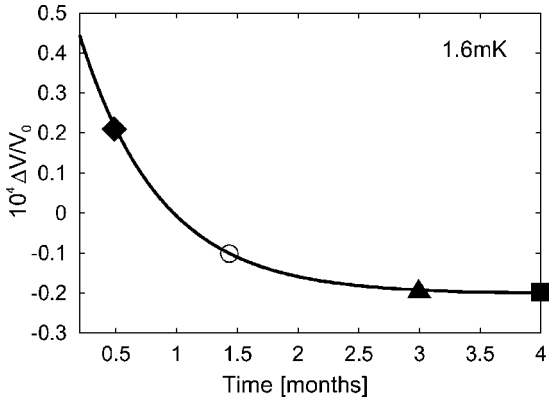

FIG. 3. The evolution of the sound velocity taken two weeks, six weeks, three months, and four months after the initial cooldown of the cryostat, all taken while the experimental plate was stabilized at 1.6 mK.

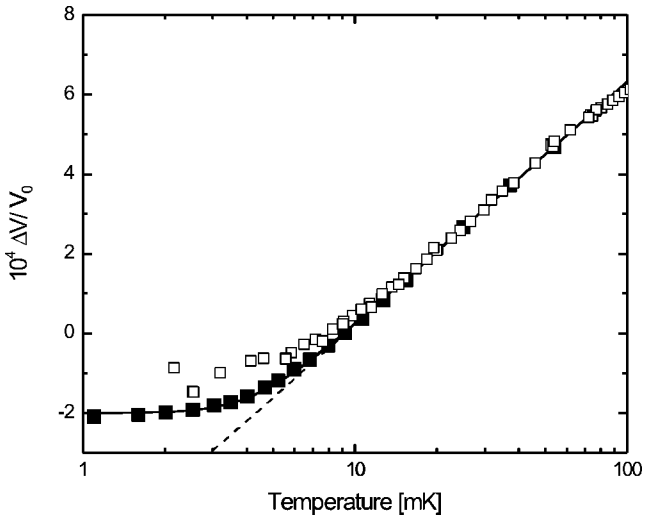

FIG. 4. Speed of sound vs experimental plate temperature on a semilogarithmic plot. Solid squares: present work; open squares: taken from Ref. 8. A logarithmic temperature dependence (dashed line) as predicted by the standard tunneling model, fits the data very well from 80 mK to ≈10 mK with a tunneling strength $C_0=2.65\times10^{-4}$; see Eq. (2). A deviation (solid curve) from the extrapolation of this temperature dependence is seen below 8 mK. Its cause is explored in the present investigation.

$\approx k_B 6.5$ mK. Its cause will be discussed in the following sections, where we explore constant inputs due to γ radiation and cosmic rays, and time dependent inputs (due to heat release) to the oscillator.

B. Heating due to γ radiation

The oscillator is sensitive to interactions with γ radiation emanating from the decay of natural radioactive atoms incorporated into building materials in the laboratory. The sensitivity manifests itself in the form of transients that cause a rapid change in the spring constant.[10] In addition, the passage of γ quanta leads to a time averaged heating of the sample. By measuring the spectrum of γ radiation captured with a Ge detector, we found[13] that the time averaged flux of γ radiation in our laboratory is $\sim 0.61\ \mathrm{cm^{-2}\,s^{-1}}$, and would hit the oscillator (surface area $\approx 5.6\ \mathrm{cm^2}$) with an average frequency of $0.09\ \mathrm{s^{-1}}$, producing an estimated ~ 13 fW steady state heat input. The residual heat input to the oscillator by γ radiation (after shielding the cryostat with 5 cm of lead) is estimated to be ≈1 fW (Ref. 13). The remaining transients observed ($\approx 0.025\ \mathrm{s^{-1}}$) were attributable to the flux of cosmic ray μ, which will be discussed in the next section.

C. Heating due to cosmic rays

The decay products of cosmic rays, muons (μ), and their decay products have "soft" and "hard" components. The soft fraction composed of β emissions and high energy γ quanta can be partially attenuated by 5 cm of lead. The results of Greisen[17] (quoted on p. 129 of Ref. 18), give the flux of the hard component as $1.27\times10^{-2}\ \mathrm{cm^{-2}\,s^{-1}}$, and the soft component as $0.52\times10^{-2}\ \mathrm{cm^{-2}\,s^{-1}}$. From geometrical considerations and the $\cos^2\theta$ (θ measured from the vertical) angular dependence of the cosmic ray flux,[13] it follows that the flux through our composite oscillator is $0.026\ \mathrm{s^{-1}} \approx 0.025\ \mathrm{s^{-1}}$, our observed count rate.

The heat deposited in the oscillator by cosmic rays is estimated as follows. The energy deposited by the passage of a μ is proportional to the mean path length, X, the density of the material, $\rho=2.2\ \mathrm{g\,cm^{-3}}$ for silica, and the collisional loss factor $[dE/d(\rho X)]$ which is approximately[18] 2 MeV $\mathrm{cm^2\,g^{-1}}$. The path length ($X=1.2$ cm) was calculated numerically, taking into account the geometry of the oscillator and the angular dependence of the μ flux. The heat deposited, P_μ, by the passage of μ is then expressed as

$$\begin{aligned} P_\mu &= [dE/d(\rho X)]\rho X \\ &= 2(\mathrm{MeV\ cm^2 g^{-1}}) \times 2.2(\mathrm{g\ cm^{-3}}) \times 1.2(\mathrm{cm}) \\ &= 850\mathrm{fJ} \end{aligned} \tag{3}$$

To calculate the average power deposited by μ, we multiply P_μ by the calculated count rate ($0.026\ \mathrm{s^{-1}}$) corresponding to a small (but not negligible) power of 22 fW.[13]

D. Strain heating experiments

In the preceding three sections, we encountered sources of heat which can raise the sample temperature. Before turning to the question of the magnitude of the temperature rise caused by this heat, we will describe in this and the following section, two sample heating experiments that were performed in which the heat input is better known. The analysis in terms of sample heating and thermal decoupling follows in Sec. IV.

As the oscillator's drive frequency is swept through resonance (see Fig. 5), the power dissipated in the a-SiO_2 sample can be estimated using the internal friction, Q^{-1} (determined at low drive amplitudes[16]) as

$$P_{strain} = (\pi^{3/16})(Q^{-1})(f_0)GV(\epsilon_a)^2, \tag{4}$$

where f_0 is the resonant frequency, ϵ_a is the strain, G is the shear modulus (3×10^{11} dynes/$\mathrm{cm^2}$) for a-SiO_2, and V is the volume of the sample ($0.26\ \mathrm{cm^3}$). This power will raise the sample's temperature and hence f_0 [see Eq. (2)]. If the temperature dependence of f_0 [or $\Delta V(T)/V_0$] is known, the temperature rise ΔT can be determined, and from this the thermal resistance R_{th} can be calculated,

$$R_{th} = \Delta T / P_{strain}. \tag{5}$$

Figure 5 shows the effect of varying ϵ_a at four temperatures. As ϵ_a increases, the resonance peak moves to higher frequencies (to the right) indicating heating. The heavy line is a theoretical fit connecting resonance frequency, f_0 and strain amplitude ϵ_a (which will be explained later) and from which R_{th} will be determined.

While this technique is useful for controlling the heat input, some shortcomings must be kept in mind: the dissipated energy depends on how much energy is absorbed from the drive force and thus on the frequency of the drive. Even if the drive voltage is large enough to heat the oscillator above

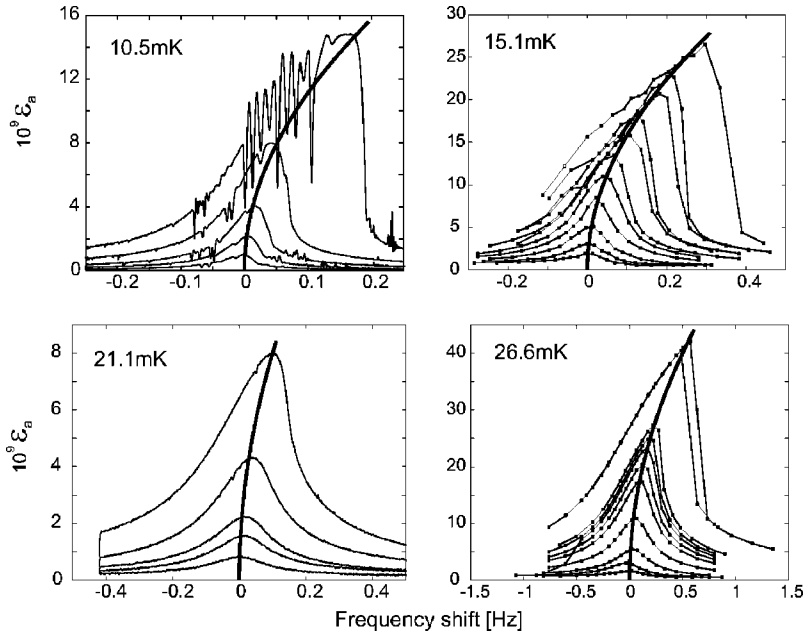

FIG. 5. The effect of strain amplitude on the frequency traces at different stage temperatures. Two left panels show the data taken as the frequency was swept through resonance as described in Sec. II B. Two right plots represent the data obtained at fixed frequencies (solid squares). The parabola intersecting at zero frequency shift is a theoretical fit; see Sec. III D and Sec. IV B. The top trace in the 21.1 mK panel represents a peak dissipation of ≈350 fW due to the internal friction of the a-SiO_2 (see Sec. III D).

ambient temperatures when the oscillator is operated on resonance, it will not absorb enough energy to heat up until the drive is near resonance. It is then possible that the oscillator "runs away" from resonance, i.e., the heat absorbed moves the resonant frequency away from the drive frequency. In turn this produces cooling, setting up a time dependent oscillation. Alternatively, if the sweep is initiated from above the resonant frequency, heating causes the resonance to rapidly "pass through" the drive frequency, and the resonance is then lost. These problems are important mainly below 10 mK for the strain amplitudes used. Another reason why the resonant drive cannot be used to heat the oscillator at the lowest temperatures is the nonlinear response of the oscillator observed below ≈5 mK, where we have seen that a higher strain amplitude causes the resonant frequency to shift to *lower* values, in a manner similar to that observed by the Heidelberg group[9] and predicted by Stockburger.[23] This behavior will be studied separately in the future. Finally, strain heating experiments become compromised below 10 mK because the place at which the dissipation occurs in the sample becomes uncertain due to the increasing relative importance of clamping losses and so the thermal resistance of the sample cannot be calculated with confidence.

Below ≈10 mK, heating was therefore carried out by γ radiation even though the spikes caused by the individual γ quanta make the determination of the frequency shift difficult. This technique is described in the next section.

E. γ heating experiments

For controlled heating by γ radiation, we used a 6.1 μCi ^{22}Na source. One of the lead bricks was removed from the shielding and the source was placed in the opening 37 cm away from the sample. In order to vary the power to the sample, sheets of lead of varying thickness were placed between the source and the sample. ^{22}Na emits 1.27 MeV and 0.511 MeV γ rays. The absorption of these quanta in Si and O is known,[24] and from this the thermal power deposited in the oscillator (sample and transducer) can be calculated. An example of heating by γ radiation is shown in Fig. 6. In these measurements the radioactive source introduces many additional transients into the frequency trace and so the determination of the resonant frequency is somewhat affected. As described in Sec. II B, particular attention was paid to the "wings" in fitting this data: on the low-frequency side of the resonance, radiation-induced "spikes" will decrease the amplitude; on the high-frequency side, it will increase it. Using this technique, the resonant frequencies could be determined with sufficient accuracy (above 3 mK, to better than the width of the resonance). The solid curves in Fig. 6 are such

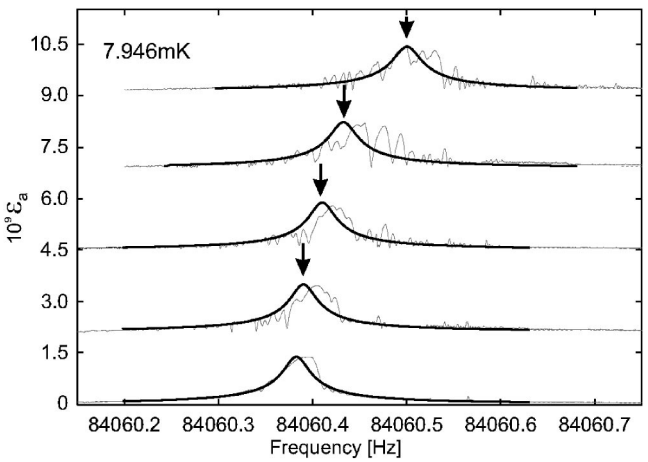

FIG. 6. Frequency traces at different gamma radiation levels [from bottom to top: no ^{22}Na+4.95 cm lead (spikes caused only by μ), ^{22}Na+3.2 cm lead, ^{22}Na+1.76 cm lead, ^{22}Na+0.8 cm lead, ^{22}Na and no intervening lead]. The Lorentzian fits emphasize the wings, in which the passage of a γ initiates a transient that shows up as a decrease below the Lorentzian, while above the resonance, transients show an increase above the expected Lorentzian response.

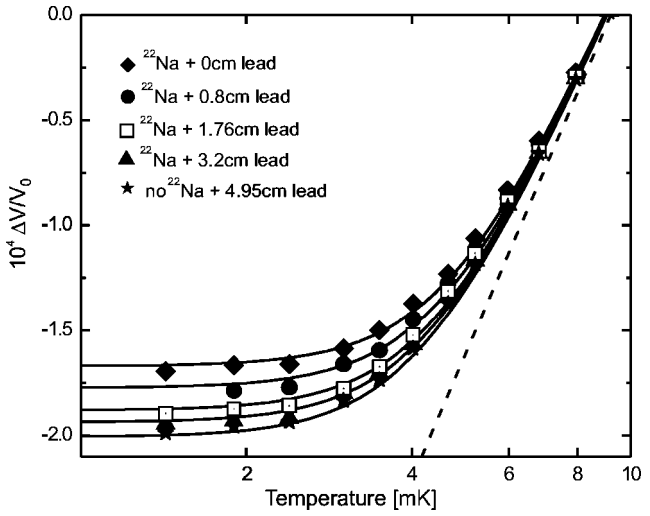

FIG. 7. Influence of γ irradiation on the speed of sound measured in thermal equilibrium three months after transferring helium, plotted against the experimental plate temperature. The radiation from the ^{22}Na source was varied with the aid of lead shields of thicknesses indicated. The solid curves are fits to the data as described in Sec. IV C. The dashed line is the same as in Figs. 2 and 4, indicating the temperature variation of $\Delta V(T)/V_0$ for a tunneling strength, $C_0=2.65\times10^{-4}$.

Lorentzian fits. As the power absorbed in the oscillator increases, the resonance peak shifts to higher temperatures. Below ~5 mK, the time to reach equilibrium increases noticeably. This additional complication is described in the next section. The equilibrated sound velocities with the γ source present and with various intervening thicknesses of lead are shown in Fig. 7 as a function of the experimental plate temperature.

F. Thermal equilibration

We now turn to the time required to thermally equilibrate the sample during (or after) γ irradiation. This time was found to become significant below an experimental plate temperature of ~5 mK. Figure 8 shows two frequency scans (taken at 500 s per scan) during cool-down after removing the radiation source. f_0 is the resonance frequency of the sample when cold. The same time dependence toward equilibrium was found after initiating the irradiation of the sample. Since the time dependence of the thermal relaxation shown in Fig. 8 cannot be determined with confidence from these traces, we define a relaxation time as the time required to reach the steady state value of the resonant frequency to within $1/e$ of its equilibrated value. These relaxation times are plotted in Fig. 9 during heating and cooling. At 4.2 mK, this relaxation time is 15 min and increases rapidly at lower temperatures until it saturates below 2 mK.

Very similar relaxation times were also observed in strain experiments during heating and cooling. It appears therefore that the relaxation is independent of the mechanism by which heat is supplied to the oscillator and is most likely connected with the tunneling states. We can only speculate that the long relaxation times indicate the existence of an additional ther-

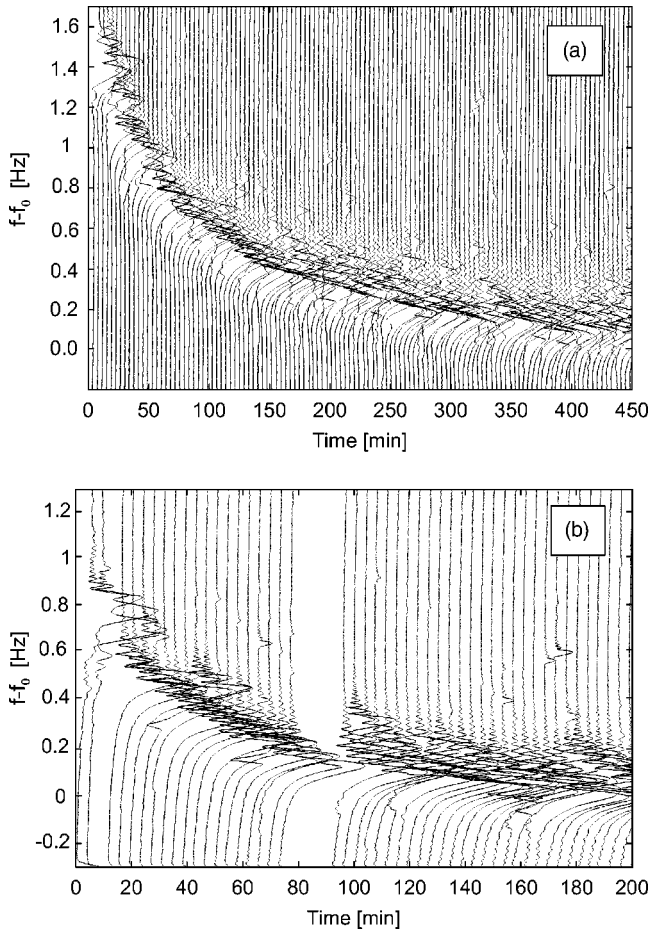

FIG. 8. Time evolution of the resonant frequency following heating by exposure to γ radiation. In the panel labeled (a), the evolution is plotted with the experimental plate held at 1.338 mK, and in the panel labeled (b), at 3.765 mK.

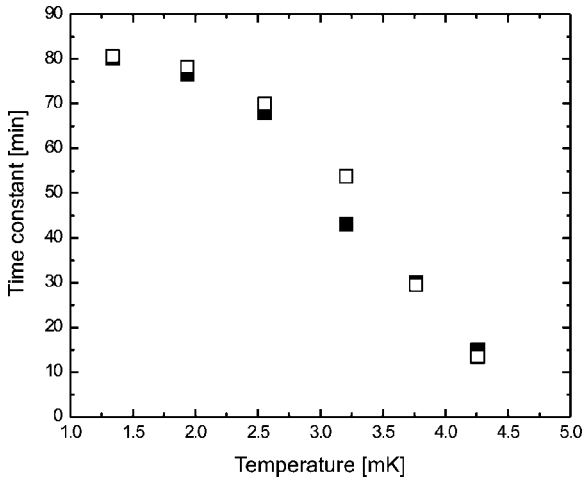

FIG. 9. Thermal relaxation time for the oscillator: open squares—following exposure of the sample to γ radiation; closed squares: relaxation time following the removal of the γ source. Temperatures are those of the experimental plate.

TABLE I. Proportionality factors a [defined in Eq. (8)] used to determine the temperature drops at the four interfaces of the mounted sample according to Cheeke *et al.* (Ref. 29). Also listed are the longitudinal and transverse speeds of sound, v_l and v_t, and the mass densities of the solids on either side of the interface needed to derive these proportionality factors.

Material/Reference	ρ (g cm^{-3})	v_l ($10^5\times$cm s^{-1})	v_l ($10^5\times$cm s^{-1})	a [K^4 (W cm^{-2})$^{-1}$]
a-SiO_2/(Ref. 2)	2.20	5.80	3.7	6.5
Stycast 2850/(Ref. 2)	2.26	4.4	2.21	7.0
Crystal quartz/(Ref. 27)	2.66	6.09	4.10	7.0
Stycast 2850/(Ref. 2)	2.26	4.4	2.21	4.0
BeCu/(Ref. 28)	8.25	4.44	2.5	

mal resistance between the TLS and the phonons.[25] However, since no detailed measurements are available at this time any further discussion on the origin of this thermal resistance is premature.

IV. DISCUSSION

We have seen in Fig. 2 that heat release within the amorphous sample leads to an elevation of the temperature dependent velocity of sound $\Delta V(T)/V_0$, the shapes at various times resembling one another. We also have seen that an intentional heat input into the sample raised the velocity, again without altering the shape of the temperature dependence (see Fig. 7). We must therefore ask by how much the data obtained without intentional heat input and after the elapse of a long time after initial cool-down (the lowest curve in Fig. 2) may have been influenced by some residual heating of the sample. In order to answer this question, we will assume, as a limiting case, that $\Delta V(T)/V_0$ follows a logarithmic behavior, as expected in the tunneling model, for $\Delta_{0,min}=0$. We will then determine whether some heat input can reproduce the measured temperature dependencies shown in Figs. 2 and 7, and providing this can be done, we will have to determine whether the heat obtained from these fits are of a reasonable magnitude.

A. Calculation of temperature increases

The calculation of the expected temperature rise of the sample for a heat input into the oscillator requires the knowledge of its thermal resistance. Phonons will be scattered by three mechanisms as they pass through the oscillator.

(a) An interaction with the tunneling states in the a-SiO_2 sample. This determines its thermal conductivity,[2]

$$\Lambda_{a\text{-}SiO_2}=\frac{1}{3}C_D v_D l,$$

$$\Lambda_{a\text{-}SiO_2}=2.6\times10^{-4}\ (\mathrm{W\ cm^{-1}\ K^{-3}})T^2, \tag{6}$$

for a-SiO_2 below 0.3 K. Here, C_D is the Debye specific heat [$C_D=1.78\times10^{-6}$ (J cm^{-3} K^{-4})T^3], and v_D the Debye velocity ($v_D=4.1\times10^5$ cm/s),[30] l is the average phonon mean free path. The validity of Eq. (6) has been established to as low as 10 mK, and according to some recent measurements on a borosilicate glass, appears to hold even down to 6 mK (Ref. 31).

(b) Casimir boundary scattering at the rough surfaces of the quartz transducer, leading to a thermal conductivity,

$$\Lambda_{Cas}=\frac{1}{3}C_v v_D d,$$

$$\Lambda_{Cas}=8.6\times10^{-2}\ (\mathrm{W\ cm^{-1}\ K^{-4}})T^3, \tag{7}$$

for our transducer. Here, C_v is the specific heat of crystalline quartz [$C_v=1.46\times10^{-6}$ (J cm^{-3} K^{-4})T^3], and v_D is the Debye velocity [$v_D=4.4\times10^5$ (cm s^{-1})],[30] and d is the diameter of the cylindrical sample (0.4 cm).

(c) Interface scattering. At low temperatures, the phonon transmission probability across the interface is determined by the acoustic mismatch which leads to a thermal boundary resistivity,

$$R_{bd}=\frac{dT}{d(PA^{-1})}=aT^{-3}, \tag{8}$$

where P is the heat flowing across the cross-sectional area A. The constant a is determined by the spectral distribution of the phonons in the two adjoining media, and by the two mass densities. Cheeke *et al.*[29] have computed tables from which the value of a can be derived for Debye solids with known speeds of sound and mass densities. In our case, four boundaries have to be considered.

From the a-SiO_2 sample to the Stycast 2850 epoxy, from the Stycast 2850 to the quartz transducer, from the quartz transducer to the epoxy, and finally from the Stycast into the BeCu base. In Table I are summarized the four constants a, together with the sound velocities and mass densities needed for their determination.

When the heat becomes large, temperature variations, and hence thermal conductivity variations along the crystalline and amorphous SiO_2 rods, together with temperature drops across the interfaces may become significant. In order to allow for that in the calculation, each rod was subdivided into 50 equal length slices. The subdivision also allows the location of the heat input to be varied as needed. Large temperature drops across interfaces were computed by integration of the inverse of Eq. (8):

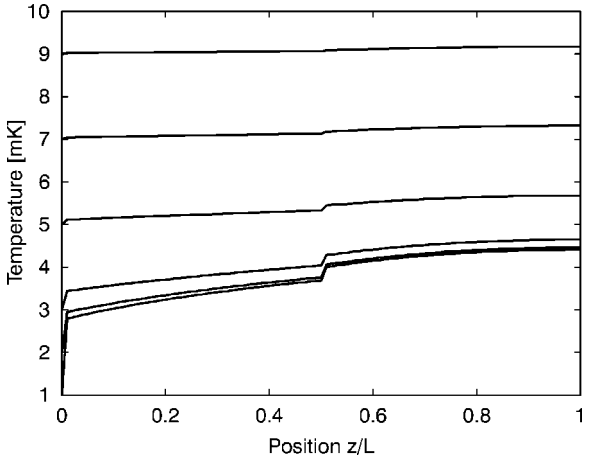

FIG. 10. The temperature profile at various temperatures starting at an experimental plate temperature of 1 mK (lowest curve), 2 mK, 3 mK, 5 mK, 7 mK, and 9 mK, respectively, for a total heat input as given in Secs. IV A and IV C. The similarity between the 1 mK and 2 mK profiles illustrates the thermal decoupling of the sample at these temperatures and would account for a temperature independent sound velocity. $z=0.5l$ denotes the boundary between the silica ($z>0.5l$) and quartz. The effective temperature of the sample is taken to be the value at $z=0.75$, the midpoint of the sample. The largest temperature drop occurs at the boundary between the quartz and the metal foot.

$$\frac{d(PA^{-1})}{dT} = \frac{T^3}{a}, \tag{9}$$

from which we obtain

$$\frac{P}{A} = (4a)^{-1}(T_2^4 - T_1^4), \tag{10}$$

where (T_2-T_1) is the temperature drop across a particular interface.

As a demonstration of how heat input will affect the temperature of the oscillator, Fig. 10 shows the temperature profiles along the oscillator for a temperature independent thermal power, $P=153$ fW, distributed uniformly throughout the a-SiO_2 sample, together with a power of 23 fW distributed uniformly over the entire oscillator, computed as described above (the reason for choosing these particular powers will be explained shortly). $z/L=0$ is the bottom of the oscillator and the location of the experimental plate, $z/L=0.5$ is the site of the transducer-sample interface. At a stage temperature of 7 mK and above, the sample temperature differs only slightly from that of the plate. At $T_{plate}=3$ mK, however, the sample temperature is noticeably higher, $\approx$4.5 mK, and varies only slightly as T_{plate} is decreased to 1 mK. With this heat input, the sample essentially decouples and does not cool below $\approx$4.5 mK, with the largest temperature drop occurring at the base.

In Secs. IV C and IV D we will combine calculations of temperature profiles of the kind shown in Fig. 10 with the temperature dependent speed of sound of the sample which we assume to vary logarithmically, as stated in the beginning of the discussion. The first question will be whether we can

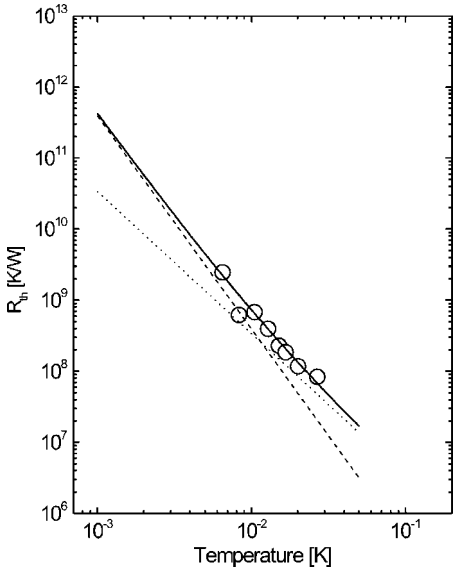

FIG. 11. The theoretically predicted thermal resistance [Eq. (14), solid curve], compared to R_{th} measured using strain heating (open circles). Also shown are dotted and dashed lines depicting the T^{-2} and T^{-3} dependencies of the silica and Casimir+boundary resistances, respectively.

reproduce the shape of the measured $\Delta V(T)/V_0$. Then we will ask whether the powers derived from such fits are physically reasonable. Before turning to this task, we will present in the next section an experimental test of the thermal resistance of the oscillator resulting from the combined effect of the three phonon scattering mechanisms introduced above.

B. Thermal resistance of the oscillator

In the previous publication,[8] measurements had been described using several thermometers that showed that the sample is in thermal equilibrium above 10 mK. We can therefore use measurements of the sound velocity, i.e., the resonance frequency, to measure the sample temperature in this temperature range. From the strain amplitude, ϵ_a, and the internal friction of the sample, Q^{-1}, we can determine the average power dissipated in the sample, and from these two quantities, determine the thermal resistance of the oscillator using Eq. (5).

In Fig. 5, the resonance is seen to shift to higher frequencies as the peak strain amplitude increases. The average power dissipated increases as the square of the peak strain amplitude. For small increases in the temperature, ΔT, the resonance frequency increases linearly with ΔT. Combining Eqs. (4) and (5), we find that $\Delta T \approx \epsilon_a^2$. The curves drawn through the resonance peaks in Fig. 5 are paraboli, from which the thermal resistance, R_{th} can be determined. In Fig. 11, these thermal resistances are shown as open circles. These measurements are compared with the thermal resistance determined from the expressions presented in Sec. IV A, and detailed below.

The thermal resistance, $R_{a\text{-}SiO_2}$, of the a-SiO_2 sample: Since the heat is developed symmetrically around the middle of the sample, the power can be considered to enter the

sample in the middle. Its thermal resistance is therefore calculated to be

$$R_{a\text{-}SiO_2} = 3.4 \times 10^4 \ (\mathrm{K}^3\,\mathrm{W}^{-1})T^{-2}. \tag{11}$$

The Casimir resistance, R_{Cas}, of the transducer is given by

$$R_{Cas} = 200 \ (\mathrm{K}^4\,\mathrm{W}^{-1})T^{-3}. \tag{12}$$

Since we may ignore the temperature variation along the oscillator at these temperatures (for the excitations used), the boundary resistance is the sum of the four interface resistances determined from the quantities a in Table I. Considering the cross sectional area of the 0.4 cm diameter rods, we obtain

$$R_{bd} = 194 \ (\mathrm{K}^4\,\mathrm{W}^{-1})T^{-3}. \tag{13}$$

The sum of these three resistances is the thermal resistance of the oscillator,

$$R_{th} = 3.4 \times 10^4 \ (\mathrm{K}^3\,\mathrm{W}^{-1})T^{-2} + 394 \ (\mathrm{K}^4\,\mathrm{W}^{-1})T^{-3}. \tag{14}$$

R_{th} is plotted as a solid curve in Fig. 11, and agrees very well with the measured data. This agreement justifies the use of the phonon scattering expressions given in the previous section for the following discussion.

C. Thermal relaxation

As the first application of the subdivided thermal resistance outlined is Sec. IV A, we attempted to fit the data in Fig. 2 showing the time dependent speed of sound, which had been tentatively explained through thermal relaxation of the tunneling states. Since it is known that the μ and γ (after shielding) deposit 23 fW uniformly distributed into the oscillator,[13] we used this power in addition to that ascribed to the thermal relaxation (this power is confined to the amorphous sample) and which was treated as an adjustable parameter.

The solid curves in Fig. 2 were obtained in this way, and fit the experimental data remarkably well. The power needed to describe the data taken two weeks after cool-down was determined to be 260 fW, and to be 165 and 153 fW for those taken after three and four months, respectively. The temperature profile in the oscillator shown in Fig. 10 is the calculated result for four months after helium transfer.

The heat release from thermal relaxation of tunneling states in amorphous solids is a well studied phenomenon,[19–21] for times not exceeding $\approx 10^2$ h. Measurements by Schwark *et al.*[20] on a sample cooled rapidly from room temperature are shown as the solid line in Fig. 12. They show the characteristic time dependence, with the power released varying as the inverse time. The magnitude decreases as the sample is allowed to relax after thermalization at temperatures lower than room temperature, as shown in the data reported by Sahling *et al.*,[21] in agreement with the tunneling model, which predicts a heat release of the following form:

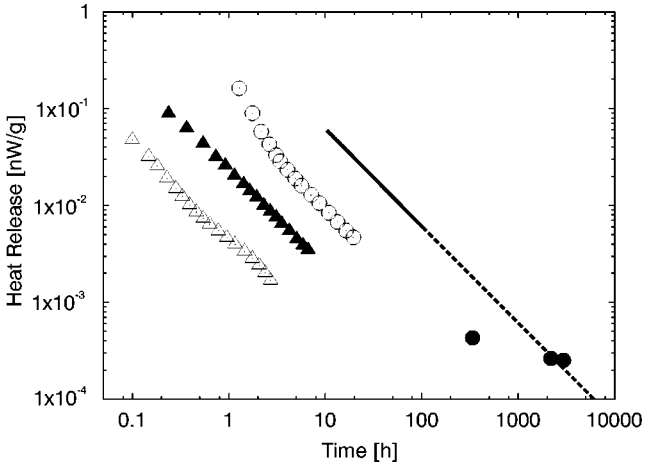

FIG. 12. Our inferred heat release (filled circles) and the results of Schwark *et al.* (Ref. 20) (solid line) obtained between 10 and 100 h and extrapolated by us (the dashed line) to ~5000 h. The data of Schwark *et al.* was obtained by cooling rapidly from room temperature to ≈20 mK. The data of Sahling *et al.* (Ref. 21) was taken at 1.34 K after cooling from 24.5 K (open circles), 3 K (filled triangles), and 2 K (open triangles).

$$P(T_h, T_c, t) = \frac{\pi^2 k_B^2}{24} \overline{P} V (T_h^2 - T_c^2) t^{-1}, \tag{15}$$

where T_h is the starting (hot) temperature, T_c is the cold temperature, t is the time after cooling the sample to T_c, V is the sample volume, and $\overline{P}$ is the spectral density of the tunneling states.

Our data, shown in Fig. 12, have a magnitude that is close to previous measurements of heat release, considering that the starting temperature T_h was not as well defined as in the earlier work, and the data were not specifically acquired with a view to exploring the time dependent heat leak. From Fig. 12, it is evident that our technique allows us to assay heat releases an order of magnitude smaller than those reported previously. The heat release in Fig. 12, and the evolution of $\Delta V(T)/V_0$ at low temperatures in Figs. 2 and 3, appears to saturate after four months, although the significance of this behavior is not clear. The heat delivered by cosmic ray μ is estimated to be 4×10^{-5} nW/g, but is $\approx 6\times$ smaller than the 2.5×10^{-4} nW/g needed to produce the saturation observed. This is a relatively small amount of "stray" heat, and could have any number of origins. Consequently, it is inappropriate to ascribe the deviation from the $\ln T$ behavior to a nonzero $\Delta_{0,min}$ without more definitive proof.

D. γ heating

The experiments shown in Fig. 7 were done on the oscillator after it relaxed for three months. The data (solid curves) can be fitted very well with our model, including a heating by μ and ambient γ radiation (23 fW) and an adjustable power $P_{\gamma,fit}$ due to γ irradiation from the ^{22}Na source, both distributed over the entire oscillator. In Table II is listed the comparison of the calculated power delivered by the γ through the different thickness lead shields (P_γ), and the

TABLE II. The table shows the calculated power (P_γ—column 2) deposited by γ from a 6.1 μCi ^{22}Na source mediated by different thicknesses (column 1) of lead sheet. We also list the power that we infer (from fits shown in Fig. 7) as being deposited by γ, $P_{\gamma\ fit}$ (column 4). In order to obtain the fits, we sum (column 3) P_γ to the power, P_{h-r} inferred as arising from heat release solely into the silica sample (three months after transferring helium) and which is deposited uniformly in the a-SiO_2 sample.

Pb (cm)	P_γ (fW)	$P_{\gamma\ fit}+P_{h-r}$ (fW)	$P_{\gamma\ fit}$ (fW)
0	109	140+165	140
0.8	42	86+165	86
1.76	16.7	37+165	37
3.2	5.6	15+165	15
4.95	0	0+165	0

power, $P_{\gamma,fit}$ used to produce the fits. The latter exceeds the former by $\approx \times 2$. Several reasons for this can be suggested: The power delivered may have been underestimated because of secondary β particles created by γ particles moving through nearby metallic parts of the cryostat. We may also have underestimated the thermal resistances at these temperatures, in particular the interfacial resistances, R_{bd}. Finally, the assumption that $\Delta V(T)/V_0$ of a-SiO_2 varies as $\ln T$ at all temperatures in our model may be an oversimplification. At present, we see no straightforward resolution of the issue, and we prefer to consider the fair agreement obtained merely as an encouraging confirmation of the model.

V. CONCLUSION

The most important observation reported here, namely that the low temperature sound velocity varies with time, calls into question our previous claim that the deviation from the logarithmic temperature dependence is linked to a low-energy cutoff of the tunneling state density, $\Delta_{0,min}$. Several of the results reported here can be reasonably well understood in terms of a picture that heat release from the relaxation of the tunneling systems is responsible for the elevation of the sample temperature, implying no such cutoff exists, although convincing proof is missing. However, the heat release does not display the expected t^{-1} time dependence and it is possible that the limiting behavior signals the presence of an unexpected stray heat leak, or of a small $\Delta_{0,min}$. Thus more work is needed to establish the time dependence and eliminate other possible explanations. On the positive side, our measurements have shown that thermal relaxation in the a-SiO_2, most likely of tunneling states, occurs even for times exceeding a thousand hours, about an order of magnitude longer than previously reported. We have also observed clear evidence that the speed of sound in a-SiO_2 varies as $\ln T$ at least to 10 and likely to 8 mK. Thus, our measurements show no evidence for a cooperative effect among the tunneling states even at these low temperatures.

ACKNOWLEDGMENTS

Support was provided by the NSF under Grant No. DMR-0202113 and No. DMR-0071630 and by the Cornell Center for Materials Research under Grant No. DMR-0079992.

[1] *Localized Excitations in Solids*, edited by R. F. Wallis (Plenum, New York, 1968).
[2] R. O. Pohl, X. Liu, and E. Thompson, Rev. Mod. Phys. **74**, 991 (2002).
[3] W. A. Phillips, Rep. Prog. Phys. **50**, 1657 (1987).
[4] P. Anderson, B. Halperin, and C. Varma, Philos. Mag. **25**, 1 (1972).
[5] *Tunneling Systems in Amorphous and Crystalline Solids*, edited by P. Esquinazi (Springer-Verlag, Berlin, 1998).
[6] J. Classen, T. Burkert, C. Enss, and S. Hunklinger, Phys. Rev. Lett. **84**, 2176 (2000).
[7] A. L. Burin, Yu. Kagan, L. A. Maksimov, and I. Ya. Polishchuk, Phys. Rev. B **69**, 220201(R) (2004).
[8] E. J. Thompson, G. Lawes, J. M. Parpia, and R. O. Pohl, Phys. Rev. Lett. **84**, 4601 (2000).
[9] J. Classen, C. Enss, and S. Hunklinger, Phys. Rev. Lett. **86**, 2480 (2001).
[10] E. Nazaretski, R. D. Merithew, V. O. Kostroun, A. T. Zehnder, R. O. Pohl, and J. M. Parpia, Phys. Rev. Lett. **92**, 245502 (2004). We note that as in this paper, the published temperatures refer to those of the experimental plate. This does not materially affect the findings described in this reference.
[11] E. Nazaretski, R. D. Merithew, R. O. Pohl, and J. M. Parpia, J. Low Temp. Phys. **134**, 407 (2004).
[12] J. M. Parpia, W. P. Kirk, P. S. Kobiela, T. L. Rhodes, Z. Olejniczak, and G. N. Parker, Rev. Sci. Instrum. **56**, 437 (1985).
[13] E. Nazaretski, V. O. Kostroun, S. Dimov, R. O. Pohl, and J. M. Parpia, J. Low Temp. Phys. **137**, 609 (2004).
[14] S. K. Watson and R. O. Pohl, Phys. Rev. B **68**, 104203 (2003).
[15] K. A. Topp, E. J. Thompson, and R. O. Pohl, Phys. Rev. B **60**, 898 (1999).
[16] E. J. Thompson, Ph.D. thesis, Cornell University, 2000.
[17] K. Greisen, Phys. Rev. **61**, 212 (1942).
[18] A. W. Wolfendale, *Cosmic Rays* (George Newnes, London, 1963), p. 40.
[19] J. Zimmermann and G. Weber, Phys. Rev. Lett. **46**, 661 (1981).
[20] M. Schwark, F. Pobell, M. Kubota, and R. M. Mueller, J. Low Temp. Phys. **58**, 171 (1985).
[21] S. Sahling, S. Abens, and T. Egert, J. Low Temp. Phys. **127**, 215 (2002).
[22] In Ref. 8 the experimental plate was heated to regulate the temperature with the dilution refrigerator providing the cooling power. The heat current set up a thermal gradient between the thermometer and the sample (e.g., the melting curve thermometer reading of 10 mK actually corresponds to a sample temperature of 11 mK). Data obtained more recently were taken with the nuclear demagnetization stage providing cooling power, while the stage was isolated from the dilution refrigerator. Thus the thermal gradient between the sample and thermometer should be minimal, since there is no additional heat flow between them.

[23] J. T. Stockburger, M. Grifoni, and M. Sassetti, Phys. Rev. B **51**, 2835 (1995).

[24] E. Storm and H. I. Israel, Nucl. Data, Sect. A **7**, 565 (1970).

[25] The expected recovery time can be estimated by evaluating the thermal time constant obtained from the product of the thermal resistance and the extrapolated heat capacity of the sample. The extrapolated thermal resistance [see Eq. (14) and Fig. 12] is 1.8×10^{10} K/W at 3 mK, while the extrapolated heat capacity (Ref. 26) is 4×10^{-10} J/K, yielding a time constant of order 10 s. At these low temperatures, the tunneling states respond with a much longer time scale, as evidenced by the slow relaxation shown in Figs. 8 and 9. Since the TLS are responsible for the low temperature elastic and thermal properties the difference between the extrapolated behavior and the experimental results suggests that there is an additional thermal impedance between the phonons and the TLS.

[26] M. Meissner and P. Strehlow, Czech. J. Phys. **46**, 2233 (1996).

[27] E. T. Swartz and R. O. Pohl, Rev. Mod. Phys. **61**, 605 (1989).

[28] Brush-Wellman Catalog, Cleveland, OH, 2002.

[29] J. D. N. Cheeke, H. Ettinger, and B. Hebral, Can. J. Phys. **54**, 1749 (1976).

[30] R. C. Zeller and R. O. Pohl, Phys. Rev. B **4**, 2029 (1971).

[31] A. Fleischmann, H.-Y. Hao, M. Neumann, and C. Enss, Physica B **329–333**, 1525 (2003).